Abdominal Imaging

Published online: 7 December 2005

Abdom Imaging (2006) 31:94–102
DOI: 10.1007/s00261-005-0047-8

Autoimmune pancreatitis: radiologic findings in 20 patients

D. H. Yang,[1] K. W. Kim,[1] T. K. Kim,[1,2] S. H. Park,[1] S. H. Kim,[1] M. H. Kim,[3] S. K. Lee,[3] A. Y. Kim,[1] P. N. Kim,[1] H. K. Ha,[1] M.-G. Lee[1]

[1]Department of Radiology, Asan Medical Center, University of Ulsan College of Medicine, 388-1, Poongnap 2-dong, Songpa-gu, Seoul 138-736, Korea
[2]Department of Medical Imaging, Toronto General Hospital, 200 Elizabeth Street, Toronto, ON, Canada
[3]Department of Internal Medicine, Asan Medical Center, University of Ulsan College of Medicine, 388-1, Poongnap 2-dong, Songpa-gu, Seoul 138-736, Korea

Abstract

Background: Autoimmune pancreatitis is a new clinical entity that is characterized by peculiar histopathologic and laboratory findings and by a dramatic clinical response to corticosteroid therapy. We evaluated the radiologic findings of autoimmune pancreatitis.
Methods: Computed tomographic, magnetic resonance imaging, endoscopic retrograde cholangiopancreatographic, and ultrasonographic findings of 20 patients with autoimmune pancreatitis in our hospital between November 2000 and December 2003 were retrospectively reviewed regarding changes and ancillary findings in the pancreatic parenchyma, the main pancreatic duct, peripancreatic vessels, and distal common bile duct. In addition, follow-up images were reviewed for changes in any abnormality seen on the initial examinations.
Results: Pancreatic parenchymal enlargement was invariably seen that was diffuse ($n = 19$) or focal ($n = 1$), with homogeneous contrast enhancement on computed tomography ($n = 20$) and magnetic resonance imaging ($n = 15$). Capsule-like rim enhancement was seen in six patients. There was focal ($n = 18$) or diffuse ($n = 2$) narrowing of the main pancreatic duct and it was usually multifocal ($n = 17$) in the former. Narrowing of the peripancreatic veins was seen in 14 patients. There was tapered ($n = 15$) or abrupt ($n = 3$) narrowing of the distal common bile duct in 18 patients, with contrast enhancement of the narrowed segment in eight. Invariably, changes in the pancreatic parenchyma, main pancreatic duct, peripancreatic vessels, and common bile duct were normalized on follow-up studies after steroid therapy.
Conclusion: In this series, common radiologic findings of autoimmune pancreatitis were (a) diffuse pancreas enlargement, (b) multifocal narrowing of the main pancreatic duct, (c) narrowing of peripancreatic veins, and (d) tapered narrowing of the distal common bile duct with frequent contrast enhancement. These findings were usually reversible with steroid therapy.

Key words: Pancreatitis—Computed tomography—Magnetic resonance—Endoscopic retrograde cholangiopancreatography—Ultrasound

Correspondence to: K. W. Kim; *email:* kimkw@amc.seoul.kr

Autoimmune pancreatitis (AIP) is a new clinical entity that is characterized by a peculiar histopathology that demonstrates marked fibrosis and lymphoplasmacytic infiltration of the pancreas, the presence of serum autoimmune phenomenon with increased serum immunoglobulin G (IgG) levels, hypergammaglobulinemia and/or positive autoantibodies, and a dramatic clinical response to corticosteroid therapy [1–4]. Unlike patients with ordinary pancreatitis, those with AIP usually present with no clinical symptoms suggesting pancreatitis or at most with only mild abdominal discomfort. Instead, AIP often manifests as obstructive jaundice and pancreatic enlargement, thereby mimicking pancreatic cancer clinically and radiologically. Because AIP is a reversible disease, it is important for radiologists to gain a perspective on it and to differentiate this entity from pancreatic cancer to avoid unnecessary surgery.

There have been occasional reports of radiologic findings of AIP [5–8]. In addition to diffuse enlargement of the pancreas and diffuse narrowing of the main pancreatic duct (MPD), it was recently reported that a capsule-like hypoattenuating rim and delayed paren-

Table 1. Clinical and laboratory findings of 20 patients with autoimmune pancreatitis

Case no. /age/sex	Symptoms	IgG (mg/dL)	IgG4 (g/L)	Autoantibodies	Amylase (IU/L)	Lipase (IU/L)	CA19.9 (ng/mL)	Total bilirubin (mg/dL)	Biopsy methods	Histopathology
1/76/M	Epigastric pain	2210[a]	0.6	−	91	70[a]	NE	2.1[a]	NE	NE
2/61/M	Palpable mass	4100[a]	NE	−	187[a]	718[a]	3	0.7	Core biopsy	+
3/57/M	Left flank pain	1990[a]	1.5	+	96	141[a]	8	0.6	Open biopsy	+
4/72/M	Jaundice	1820[a]	NE	+	55	14	21	2[a]	Core biopsy	+
5/62/M	Jaundice	1930[a]	NE	+	18	21	149[a]	20.5[a]	Core biopsy	+
6/60/M	Jaundice	1880[a]	3.3[a]	−	46	39	25	13.5[a]	Open biopsy	+
7/69/M	Indigestion	2010[a]	1.1	−	NE	NE	3	1.0	Open biopsy	+
8/42/M	Epigastric pain	1730[a]	0.1	−	75	37	18	5.2[a]	Core biopsy	+
9/68/M	Jaundice	1920[a]	2.6[a]	−	169[a]	283[a]	4	11.9[a]	Whipple operation	+
10/69/M	Jaundice	3555[a]	13.6[a]	−	68	79[a]	50[a]	15.4[a]	NE	NE
11/54/M	Weight loss	2100[a]	NE	NE	52	45	14	6.2[a]	NE	NE
12/46/M	Weight loss	1470	NE	−	22	22	3	1.6[a]	Core biopsy	+
13/64/M	Epigastric pain	1440	NE	+	273[a]	527[a]	33	6.7[a]	Core biopsy	+
14/61/M	Epigastric pain	1230	8.4[a]	+	46	22	24	2.9[a]	Core biopsy	+
15/46/M	Jaundice	1110	0.4	−	40	14	16	3.2[a]	Core biopsy	+
16/65/F	Epigastric pain	1200	1.1	−	160[a]	156[a]	466[a]	1.1	Core biopsy	+
17/62/M	Weight loss	1500	1.9[a]	−	48	58[a]	30	10.4[a]	Core biopsy	+
18/52/M	Epigastric pain	1570	3.1[a]	NE	66	72	22	10.8[a]	Open biopsy	+
19/54/F	Jaundice	1240	0.3	−	28	35	28	8.3[a]	Core biopsy	+
20/57/M	Jaundice	1490	2.5[a]	−	35	54	291[a]	15.3[a]	Whipple operation	+

[a]Serum level higher than normal
−, negative result; +, positive result; F, female; M, male; NE, not examined; Ig, immunoglobulin

chymal enhancement on computed tomography (CT) and magnetic resonance (MR) imaging appear to be the characteristic findings of AIP [5, 6]. However, with a continued increase in the number of the cases being reported, it has become clear that focal-type AIP may also exist, and it seems that the small number of patients included in previous studies preclude an assessment of the frequency of these findings. During the past 3 years, we have found 20 patients with AIP in which radiologic studies, including CT, endoscopic retrograde cholangiopancreatography (ERCP), and sometimes MR imaging and ultrasonography (US), were available for review. Therefore, the purpose of this report is to describe the radiologic findings of AIP.

Materials and methods

Patients

A computer search of our institution's pathology, radiology, and medical records between November 2000 and December 2003 showed 20 consecutive patients who were diagnosed with AIP and underwent cross-sectional imaging studies at the time of diagnoses and during the follow-up period. The clinical diagnosis of AIP was made on the basis of the modified diagnostic criteria proposed by the Japan Pancreas Society [9]: narrowing or obstruction of the MPD and an enlarged pancreas in the area corresponding to MPD changes on imaging studies, increasing serum levels of IgG (or subclass IgG4) or positive antinuclear antibody, and lymphoplasmacytic infiltration and fibrosis in pancreatic tissues. Twelve of 20 patients fulfilled these criteria. Another six patients met at least criterion 2 ($n = 2$) or 3 ($n = 4$) in addition to fulfilling criterion 1. The other two patients fulfilled criteria 2 and 3.

The clinical findings of patients with AIP are summarized in Table 1. There were 18 men and two women, with an age range of 42 to 76 years (mean 60 years). Usually, patients with AIP exhibited jaundice and complained of vague abdominal symptoms. Levels of serum amylase and lipase were normal in 50% of these patients, and total bilirubin level was high in 80%. Association with other autoimmune diseases was found in one patient who had Sjögren syndrome. Eighteen of 20 patients were treated with 30 to 40 mg of oral prednisolone (Delta Cotef; Pharmacia Korea, Gyeonggi, Korea) and were followed for 4 to 37 months (mean 16 months). In all patients, subjective symptoms and laboratory abnormalities were normalized within 2 months. After confirming clinical improvement, the corticosteroid dose was tapered to a maintenance dose (5 to 10 mg). In one patient, recurrent symptoms and laboratory abnormalities were found 5 months after tapering the corticosteroid. One month after retreatment with 40 mg of oral prednisolone, clinical findings improved.

All 20 patients underwent CT and ERCP examination at initial presentation. MR imaging and US examinations were also performed in 15 and 16, respectively. Eighteen patients underwent follow-up imaging studies (CT, $n = 18$; ERCP, $n = 17$; and MR imaging, $n = 2$) after steroid therapy.

Imaging protocols

CT scans were obtained by using a multislice helical CT scanner (LightSpeed QX/I, GE Medical Systems,

Milwaukee, WI, USA, $n = 14$) or single-slice helical CT scanners (HiSpeed, GE Medical Systems, $n = 3$; or Somatom Plus-4, Siemens Medical Systems, Erlangen, Germany, $n = 3$). Each patient received 120 to 150 mL of iopromide (Ultravist 370, Schering, Berlin, Germany) through an 18-gauge angiographic catheter inserted into an antecubital vein using a power injector (LF CT 9000, Liebel-Flarsheim, Cincinnati, OH, USA) at a rate of 3 mL/s. Contrast-enhanced CT scans were obtained using a biphasic protocol during the arterial phase (AP) and portal venous phase (PVP) in 17 patients and a monophasic protocol during the PVP in the other three. With multislice helical CT, AP imaging (collimation 1.25 mm, pitch 6:1) was initiated within 10 s after enhancement of the descending aorta reached 100 HU, as measured by a bolus tracking technique (Smart Prep, GE Medical Systems). PVP images were obtained 45 s after completion of AP scanning (collimation 2.5 mm, pitch 6:1). With the single-slice helical CT scanners, AP and PVP images were obtained 36 and 72 s after contrast injection, respectively (collimation 5 mm, pitch 1.4). Noncontrast CT scans were included in 19 patients.

ERCP examination was performed by two gastroenterologists who used conscious sedation under fluoroscopy. After cannulation of the bile duct and the pancreatic duct, multiple views of these ducts using different projections were obtained after injection of 10 to 30 mL of water-soluble contrast under fluoroscopic control to demonstrate the entire ductal anatomy and any pathology.

MR examinations were performed on a 1.5-T MR system (Magnetom Vision, Siemens Medical Systems). Axial T1-weighted images were obtained by using a fast low-angle shot (FLASH) sequence with the following parameters: 149 ms repetition time (TR), 4.1 ms echo time (TE), flip angle of 80°, 19-s breath hold; 19 sections, section thickness of 8 mm (intersection gap of 2 mm), field of view (FOV) of 350 mm, and 132 × 256 matrix. Axial T2-weighted images were obtained with half-Fourier acquisition single-shot turbo spin-echo sequences. The parameters were TR of infinity, effective TE of 134 ms, echo spacing of 4.6 ms, an echo-train length of 104, flip angle of 150°, 20-s breath hold, 19 sections, section thickness of 8 mm (2-mm gap), FOV of 350 mm, and 192 × 256 matrix. Two different MR cholangiopancreatography techniques were applied, i.e., single-slab heavily T2-weighted thick-section imaging (rapid acquisition with relaxation enhancement; TR infinity, TE 1200 ms, flip angle 150°, 50- to 90-mm slab thickness, FOV 300 mm, one signal acquired) and a multislice half-Fourier acquisition single-shot turbo spin-echo sequence (TR infinity, TE 95 ms, flip angle 150°, 4-mm section thickness with no gap, 13 to 15 slices). MR angiography was performed in the coronal plane using a three-dimensional FLASH sequence (TR 4.6 ms, TE 1.8 ms, flip angle 30°, 120-mm slab thickness, FOV 400 mm, 32 partitions, 200 × 512 matrix). Using a test bolus method, the peak arterial enhancement time was calculated and the AP of MR angiography was obtained after administration of 30 mL (0.2 mmol/kg) of gadopentetate dimeglumine (Magnevist, Schering) with a power injector at a rate of 4 mL/s followed by 10 mL of saline flush. The AP images were systematically subtracted from the precontrast images. PVP scanning was begun with an interscan delay of 20 s after AP scanning. Maximum intensity projection angiograms with coronal, oblique coronal, and sagittal projections were generated using AP and PVP images, respectively. Delayed contrast-enhanced axial images were obtained with fat-suppressed FLASH (parameters were the same as those of the unenhanced T1 sequence) 5 min after administration of gadopentetate dimeglumine.

US examinations were performed by five radiologists, with special attention given to the presence or absence of abnormalities in the pancreas and the biliary tree. Various commercially available scanners (Sequoia, Acuson, Mountain View, CA, USA, $n = 4$; HDI 3000, ATL, Bothell, WA, USA, $n = 8$; LOGIQ 700, GE Medical Systems, $n = 4$) were used, and the scanning was performed with 2- to 5-MHz convex transducers.

Follow-up CT, ERCP, and MR imaging were performed in the same manner as the imaging protocol at the initial presentation.

Image analyses

Three radiologists retrospectively evaluated all images for the following items using picture archiving and communication system workstation monitor. They were aware of the purpose of this study and conclusions were made by means of consensus.

First, changes in the pancreatic parenchyma (size, attenuation, signal intensity or echogenicity, enhancement pattern, and the presence or absence of focal lesion) were assessed on CT, MR, and US. To determine the size of the pancreas, we measured the longest transverse diameter of the pancreatic head, body, and tail on CT. The CT attenuation, MR signal intensity, and degree of contrast enhancement of the pancreatic parenchyma on CT and MR images were compared with those of the liver seen at the same level. The echogenicity of the pancreas on US was compared with that of peripancreatic fat tissue. The focal lesion of the pancreas was defined as any intrapancreatic lesion showing different attenuation, signal intensity, or echogenicity on imaging studies. In addition, the presence or absence of a capsule-like rim surrounding the pancreas was assessed. Second, MPD changes were assessed on ERCP. The presence or absence of complete ductal occlusion was evaluated. We categorized the pattern of MPD narrowing into diffuse and focal types. The diffuse type was defined as narrowing of the entire MPD compared with the normal

caliber. The focal type was defined as a focally narrowed MPD with a variable number and location. Number and location (head, neck and body, and tail) of focal MPD narrowing were evaluated. In each case, the maximal caliber of the MPD was measured. Third, the presence or absence of peripancreatic vessel narrowing or thrombosis was assessed on contrast-enhanced CT and MR angiography. Fourth, the presence or absence of narrowing of the distal common bile duct (CBD) and, if any, the length of the narrowed segment were assessed on MR cholangiopancreatography and ERCP. These features were subjectively graded as tapered or abrupt narrowing according to the morphologic appearance of the proximal duct. The presence or absence of contrast enhancement of the narrowed segment was also assessed on contrast-enhanced CT and MR images. Fifth, the reviewers evaluated the combined ancillary findings, including the presence or absence of parenchymal calcification, peripancreatic infiltration, pseudocyst, peripancreatic lymph node enlargement, retroperitoneal fibrosis, and ascites. The peripancreatic infiltration was categorized as being of a mild or severe degree; mild degree was defined as a diameter of infiltration no larger than 1 cm, and severe degree was defined as a diameter larger than 1 cm. The peripancreatic lymph node was considered to be enlarged when it was larger than 1 cm in its short diameter.

Follow-up CT, ERCP, and MR images were evaluated for change of any abnormality seen on the initial examination. Of these changes, those in the size of the pancreas between the initial and follow-up CT scans were analyzed for a statistical difference by using the Wilcoxon signed rank test.

Results

The principal radiologic findings of AIP are summarized in Table 2.

Pancreatic parenchyma

In all patients, the pancreatic parenchyma showed diffuse or focal swelling on CT, MR imaging, and US. In 19 patients (95%), there was no focal mass in the pancreatic parenchyma (Fig. 1). A focal mass-like lesion was found in only one patient (5%). The longest transverse mean diameters of the pancreatic head, body, and tail were 37 ± 6 mm, 25 ± 4 mm, and 30 ± 6 mm, respectively. Usually, the pancreatic parenchyma showed isoattenuation or high attenuation compared with liver on AP and PVP CT scans. Of the 11 patients who had fat-suppressed T1-weighted images, the pancreatic parenchyma showed low signal intensity in nine (82%) and isoattenuation signal in two (18%). Of the 15 patients who had T2-weighted images, the pancreatic parenchyma showed high signal in 13 (87%) and isoattenuation signal in two (13%). Of the 14 patients with gadolinium-enhanced T1-weighted images, 12 (86%) showed high signal intensity compared with the liver. Invariably, the pancreatic parenchyma showed homogeneous low echogenicity on US. The enhancement pattern of the pancreatic parenchyma was homogeneous in all patients on CT and MR images.

In six of 20 patients (30%), a capsule-like low attenuation rim was seen surrounding the pancreas on contrast-enhanced CT. Of the four patients who underwent MR imaging, this finding was seen in only two patients on gadolinium-enhanced T1-weighted images. Further, this capsule-like structure was not noted on unenhanced MR imaging (Fig. 2).

MPD changes

There was no instance of complete occlusion of the MPD. MPD narrowing was focal in 18 patients (90%; Fig. 1) and diffuse in the other two (10%; Fig. 3). In the focal type, MPD narrowing was usually multiple (60%) and seen in all segments of the pancreas. In five patients (25%), MPD narrowing was noted in only one segment of the pancreas. The maximal caliber of the MPD ranged from 2 to 5 mm (mean 3 mm).

Peripancreatic vessels

In 14 patients (70%), peripancreatic vein narrowing was noted (Fig. 1C). Narrowing of the superior mesenteric vein, splenic vein, main portal vein, and left renal vein was seen in 10 patients (50%), 12 patients (60%), one patient (5%), and one patient (5%), respectively. However, none had visible thrombus or complete occlusion of any of these veins. Arterial narrowing was not observed.

Bile duct

There was narrowing of the distal CBD in 18 patients (90%). The length of the narrowed segment ranged from 10 to 40 mm (mean 30 mm). Tapered luminal narrowing was seen in 15 patients (83%), and abrupt narrowing was seen in the other three (17%). Enhancement of the narrowed segment was seen in eight patients (44%) on contrast-enhanced CT and MR images (Fig. 4).

Ancillary findings

A mild degree of peripancreatic infiltration was seen in seven patients (35%). However, no patient had severe peripancreatic infiltration. Also, none showed parenchymal calcification, pseudocyst, peripancreatic lymph node enlargement, or ascites. In one patient, benign retroperitoneal fibrosis was found on CT scan.

Table 2. Principal radiologic findings in 20 patients with autoimmune pancreatitis

	Changes of pancreas parenchyma										Main pancreatic duct narrowing		Distal common bile duct narrowing		
		CT attenuation			MRI signal intensity				Low density or signal intensity rim on CT/MRI						
Case no.	Swelling	Precontrast	Arterial phase	Portal phase	T1	T2	Gd-T1	Echogenicity on US	CT	MRI	Involving site	Type	Shape	Enhancement	Stenosis of peripancreatic vein
1	Diffuse	Iso	NA	High	NA	NA	NA	NA	−	NA	All	Focal	Tapered	−	−
2	Diffuse	Low	Iso	Iso	NA	High	High	Low	−	−	All	Focal	NI	−	+
3	Diffuse	NA	NA	Low	NA	NA	NA	Low	+	NA	Body, tail	Focal	Abrupt	−	+
4	Diffuse	Low	Iso	Iso	Low	High	High	Low	−	−	All	Focal	Tapered	+	+
5	Diffuse	Low	Iso	Iso	Low	High	High	Low	+	−	All	Focal	Abrupt	+	+
6	Diffuse	Iso	Iso	Iso	NA	High	High	NA	+	−	Tail	Focal	Tapered	−	−
7	Diffuse	Low	High	Iso	NA	Iso	Iso	Low	−	−	All	Focal	Tapered	+	−
8	Focal	Low	Low	Low	Iso	Iso	High	Low	−	−	Head	Focal	Tapered	+	−
9	Diffuse	Low	High	Iso	Low	High	High	Low	−	−	Head	Focal	Tapered	+	+
10	Diffuse	Iso	NA	Iso	NA	NA	NA	Low	+	NA	All	Focal	Tapered	−	−
11	Diffuse	Low	High	High	Low	High	High	Low	+	+	All	Focal	Tapered	+	+
12	Diffuse	Low	Low	Iso	Low	High	High	Low	+	+	All	Focal	NI	−	+
13	Diffuse	Iso	Iso	Iso	NA	High	High	NA	−	−	All	Focal	Tapered	−	+
14	Diffuse	Iso	Iso	Iso	Low	High	High	Low	−	−	All	Focal	Tapered	+	+
15	Diffuse	Low	Low	Low	NA	NA	NA	Low	−	NA	All	Focal	Abrupt	−	+
16	Diffuse	Iso	Iso	Iso	Iso	High	NA	Low	−	−	All	Diffuse	Tapered	−	+
17	Diffuse	Iso	Iso	Iso	Low	High	High	Low	−	−	Tail	Focal	Tapered	−	−
18	Diffuse	Low	Iso	Iso	Low	High	High	NA	−	−	All	Diffuse	Tapered	−	+
19	Diffuse	Low	High	High	NA	NA	NA	Low	−	NA	All	Focal	Tapered	−	+
20	Diffuse	Iso	Iso	Iso	Low	High	Iso	Low	−	−	Head	Focal	Tapered	+	+

−, negative result; +, positive result; CT, computed tomography; High, high attenuation or signal intensity on CT/MRI; Iso, equal attenuation or signal intensity on CT/MRI; Low, low attenuation or signal intensity on CT/MRI; MRI, magnetic resonance imaging; NA, not available; NI, did not involve the bile duct; T1, fat-suppressed T1-weighted imaging

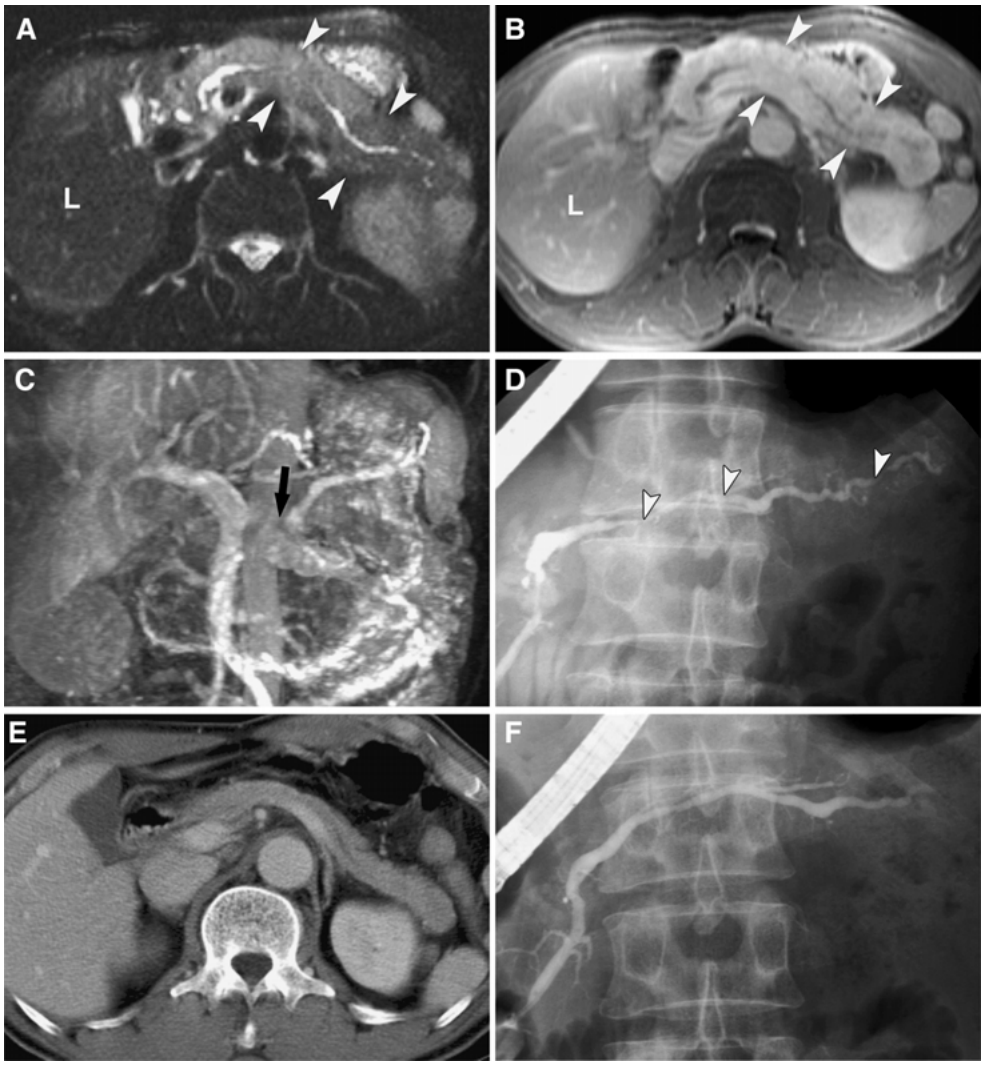

Fig. 1. AIP in a 61-year-old man that presented as a palpable abdominal mass for 6 months. **A** Transverse T2-weighted MR image shows diffuse enlargement of the pancreas (*arrowheads*). Note the high signal intensity of the pancreatic parenchyma compared with that of liver (*L*). **B** Contrast-enhanced MR image shows stronger enhancement of the pancreatic parenchyma (*arrowheads*) compared with the liver (*L*). **C** Maximal intensity projection image generated from MR angiography during the PVP shows severe narrowing of the splenic vein (*arrow*). **D** ERCP image shows multiple narrowings of the main pancreatic duct (*arrowheads*) involving all segments of the pancreas. **E** On contrast-enhanced CT obtained 2 months after steroid therapy, enlargement of the pancreas has decreased. **F** On follow-up ERCP obtained 2 months after steroid therapy, narrowing of the pancreatic duct has decreased.

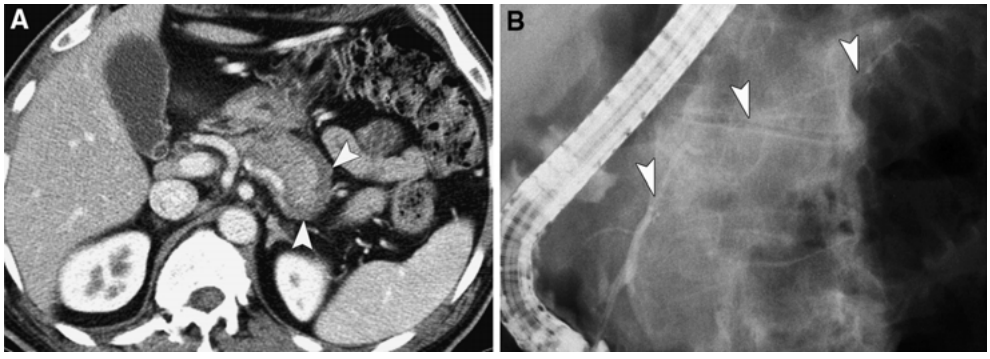

Fig. 2. AIP in a 46-year-old man that presenting as jaundice for 8 months. **A** Contrast-enhanced transverse CT scan shows the low attenuation rim (*arrowheads*) in the pancreas tail. **B** ERCP image shows multiple narrowings of the main pancreatic duct (*arrowheads*) involving all segments of the pancreas.

Follow-up images

On follow-up CT images (mean interval from initial CT, 2 months; range 1–8 months), the longest diameters of the pancreatic head, body, and tail were significantly decreased ($p \leq 0.001$). The longest mean diameters of the head, body, and tail were 26 ± 5 mm, 16 ± 4 mm, and 17 ± 6 mm, respectively. In all patients, morphologic change in the MPD was normalized on follow-up ERCP (mean interval from initial ERCP, 2 months; range 1–4 months). In one patient with recurrence, narrowing of the MPD was seen in the pancreatic tail. Narrowing of the distal CBD decreased in all patients. In 11 of 18 patients, an endoscopic plastic biliary stent

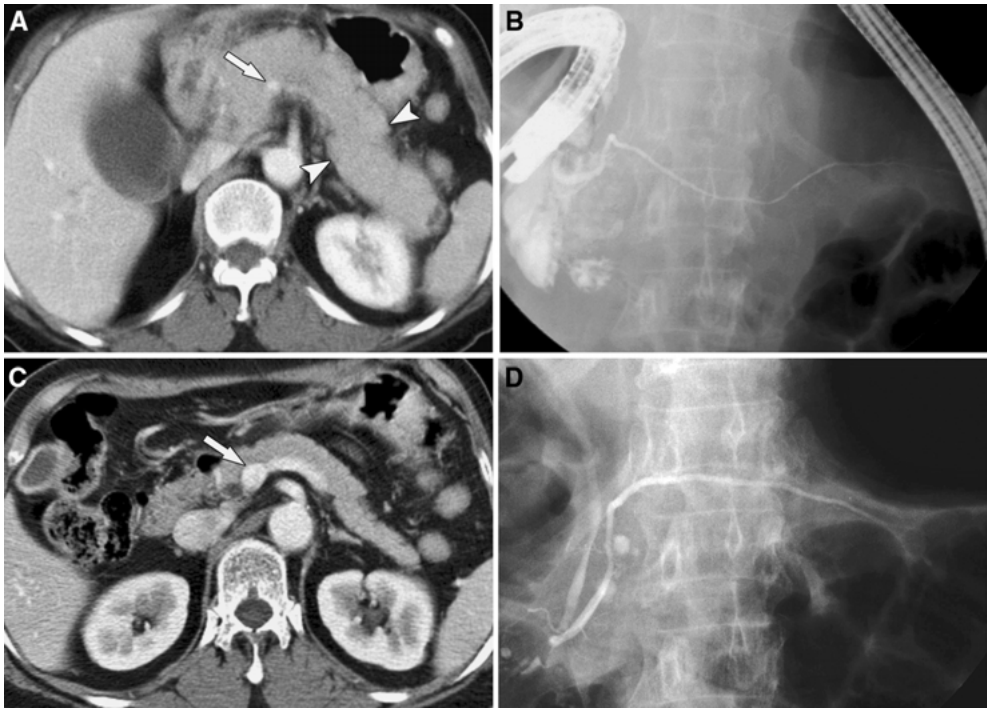

Fig. 3. AIP in a 65-year-old woman that presented as epigastric pain for 4 months. **A** Contrast-enhanced CT image shows diffuse enlargement of the pancreas (*arrowheads*). Narrowing of the portal confluence portion (*arrow*) is noted. **B** ERCP image shows diffuse narrowing of the main pancreatic duct throughout the entire pancreas. **C** On contrast-enhanced CT obtained 2 months after steroid therapy, enlargement of the pancreas has decreased. Narrowing of the portal confluence (*arrow*) has also decreased. **D** On ERCP images obtained 2 months after steroid therapy, diffuse narrowing of the main pancreatic duct has decreased.

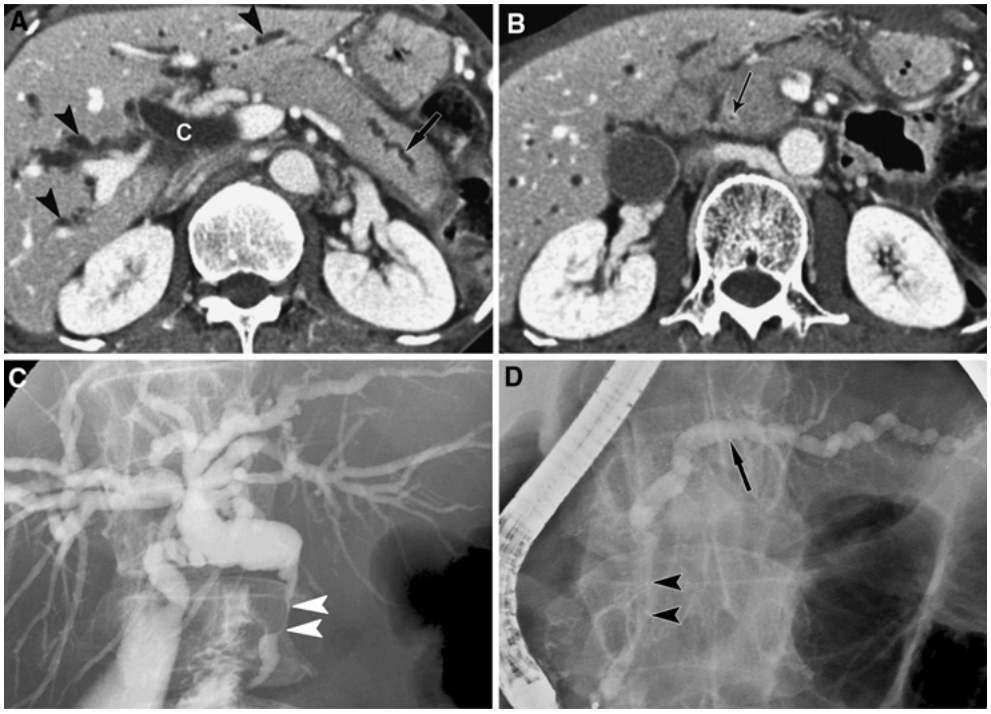

Fig. 4. AIP in a 68-year-old man that presented as jaundice for 8 months. **A** Contrast-enhanced transverse CT scan shows diffuse swelling of the pancreas. Both intrahepatic bile ducts (*arrowheads*) and the CBD (*C*) are diffusely dilated. Note dilatation of the main pancreatic duct (*arrow*). **B** Contrast-enhanced transverse CT scan shows narrowing and concentric wall thickening of the distal CBD with strong contrast enhancement (*arrow*). **C** Percutaneous direct cholangiogram shows diffuse dilatation of the intrahepatic bile duct and the CBD. The distal CBD is abruptly narrowed (*arrowheads*). **D** ERCP image shows focal narrowing of the main pancreatic duct in the head portion (*arrowheads*). Note dilatation of the upstream pancreatic duct (*arrow*).

(Natick 10F, Boston Scientific, Natick, MA, USA) was placed. All stents were successfully removed during follow-up ERCP after steroid therapy. In addition, narrowing of the peripancreatic vein decreased in all patients.

Discussion

Since Yoshida et al. [1] proposed the entity of AIP, similar cases have been reported [2–8]; however, the diagnostic criteria of AIP are still being debated and continue to evolve [10]. Recently, the Japan Pancreas Society proposed three diagnostic criteria for AIP, i.e., pancreatic imaging, laboratory data, and histopathologic findings [9]. According to these criteria, pancreatic imaging is a most important and consistent item because laboratory findings and pathologic examination are often insufficient and sometimes nonspecific for the diagnosis of AIP. For example, the level of serum IgG is normal in 24% of patients with AIP, and increased IgG4 is not specific for AIP [8, 10]. Mild lymphoplasmacytic infiltration and fibrotic change of pancreatic parenchyma are also found in patients with chronic alcoholic pancreatitis [11]. However, pancreatic imaging findings as a criterion of AIP have also been controversial. Some investigators do not agree with the Japanese criteria [10] and prefer the following criteria for the diagnosis of AIP: histology and cytology, an association with other postulated autoimmune diseases particularly of the gastrointestinal tract, and response to steroid therapy.

The principal radiologic findings of AIP in our study were similar to the results of previous reports [5–8, 10]. CT, MR imaging, and US invariably demonstrated diffuse enlargement of the pancreas. ERCP images usually showed focal or diffuse narrowing of the MPD. Narrowing of the distal CBD and the peripancreatic vessels was also commonly observed. Pancreatic calcification or pseudocyst was not observed. However, some findings of our study were quite different from those of previous studies. The low density or signal intensity rim on contrast-enhanced CT and MR imaging, which were thought to be characteristic of AIP, were observed in only 30% of our patients. This capsule-like structure was not usually noted on T1- or T2-weighed MR imaging.

It is interesting to note that eight of our patients showed enhancement in the narrowed segment of the distal CBD on contrast-enhanced CT and MR imaging. Hyodo et al. [12] reported findings on contrast-enhanced intraductal US of a thickened bile duct wall. They reported that strong enhancement on intraductal US was characteristic of AIP. However, enhancement of a narrowed duct on CT and MR imaging had not been reported before our study. An awareness of this finding is important because it may suggest the possibility of malignancy. In our study, one patient who presented duct enhancement was suspected of having distal CBD cancer; this patient subsequently underwent a Whipple procedure (Fig. 4).

With an increase in the number of reported cases, the rare manifestation of AIP has been reported. Retroperitoneal fibrosis combined with AIP is very rare and only few cases have been reported [10, 13–15]. Awareness of this finding may prevent inappropriate surgery because many retroperitoneal processes such as lymphoma or carcinoma of a retroperitoneal organ may produce similar imaging findings. A focal mass-forming type of AIP has also been reported in several studies [16–19]. In those cases, AIP can be diagnosed based on abnormal laboratory findings and the results of percutaneous needle aspiration biopsy. However, adequate imaging criteria to differentiate AIP from pancreatic cancer have not been established.

Because the clinical manifestation of AIP usually mimics that of pancreas cancer, radiologic differentiation of AIP from pancreas cancer is very important. Based on the results of our study, we believe that several points may be helpful in differentiating AIP from pancreatic cancer. First, there is usually diffuse pancreatic enlargement in AIP with homogeneous contrast enhancement. Second, although the MPD may show multifocal or diffuse narrowing in patients with AIP, complete occlusion of the MPD or upstream pancreatic duct dilatation is unlikely. However, differentiating the mass-forming or focal swollen type of AIP from pancreatic cancer remains problematic. Wakabayashi et al. [20] reported that the following imaging findings are useful in the differentiation of focal-type AIP from pancreatic cancer: the stenosed MPD is longer than 30 mm and the upstream MPD is smaller than 6 mm in diameter on ERCP. In our series, the maximum diameter of the upstream MPD was smaller than 5 mm in all patients. Third, although the peripancreatic vein may be involved in patients who have AIP, involvement of the peripancreatic artery is unlikely.

In our series, common radiologic findings of AIP can be summarized as follows: (a) diffuse enlargement of the pancreatic parenchyma without a focal lesion on CT and MR imaging; (b) multifocal narrowing of the MPD; (c) narrowing of the peripancreatic veins; (d) tapered narrowing of the distal CBD with frequent contrast enhancement; (e) lack of lymphadenopathy, peripancreatic infiltration, pseudocyst, ascites, and parenchymal calcification; and (f) normalization of radiologic abnormalities after steroid therapy. Recognizing these findings is very important to arrive at the correct diagnosis of AIP and thus prevent unnecessary invasive procedures or surgery.

References

1. Yoshida K, Toki F, Takeuchi T, et al. (1995) Chronic pancreatitis caused by an autoimmune abnormality. Proposal of the concept of autoimmune pancreatitis. Dig Dis Sci 40:1561–1568
2. Ito T, Nakano I, Koyanagi S, et al. (1997) Autoimmune pancreatitis as a new clinical entity. Three cases of autoimmune pancreatitis with effective steroid therapy. Dig Dis Sci 42:1458–1468

3. Okazaki K, Chiba T (2002) Autoimmune related pancreatitis. Gut 51:1–4
4. Okazaki K, Uchida K, Chiba T (2001) Recent concept of autoimmune-related pancreatitis. J Gastroenterol 36:293–302
5. Irie H, Honda H, Baba S, et al. (1998) Autoimmune pancreatitis: CT and MR characteristics. AJR 170:1323–1327
6. Furukawa N, Muranaka T, Yasumori K, et al. (1998) Autoimmune pancreatitis: radiologic findings in three histologically proven cases. J Comput Assist Tomogr 22:880–883
7. Horiuchi A, Kawa S, Hamano H, et al. (2002) ERCP features in 27 patients with autoimmune pancreatitis. Gastrointest Endosc 55:494–499
8. Horiuchi A, Kawa S, Akamatsu T, et al. (1998) Characteristic pancreatic duct appearance in autoimmune chronic pancreatitis: a cast report and review of the Japanese literature. Am J Gastroenterol 93:260–263
9. Japan Pancreas Society (2002) Diagnostic criteria for autoimmune pancreatitis 2002. J Jpn Pancreas Soc 17:585–587
10. Pearson RK, Longnecker DS, Chari ST, et al. (2003) Controversies in clinical pancreatology: autoimmune pancreatitis: does it exist? Pancreas 27:1–13
11. Ectors N, Maillet B, Aerts R, et al. (1997) Non-alcoholic duct destructive chronic pancreatitis. Gut 41:263–268
12. Hyodo T, Hyodo N (2003) Ultrasonographic evaluation in patients with autoimmune-related pancreatitis. J Gastroenterol 38:1155–1161
13. Fukukura Y, Fujiyoshi F, Nakamura F, et al. (2003) Autoimmune pancreatitis associated with idiopathic retroperitoneal fibrosis. AJR 181:993–995
14. Hamano H, Kawa S, Ochi Y, et al. (2002) Hydronephrosis associated with retroperitoneal fibrosis and sclerosing pancreatitis. Lancet 359:1403–1404
15. Uchida K, Okazaki K, Asada M, et al. (2003) Case of chronic pancreatitis involving an autoimmune mechanism that extended to retroperitoneal fibrosis. Pancreas 26:92–94
16. Taniguchi T, Seko S, Azuma K, et al. (2000) Autoimmune pancreatitis detected as a mass in the tail of the pancreas. J Gastroenterol Hepatol 15:461–464
17. Venu RP, Radke JS, Brown RD, et al. (1999) Autoimmune pancreatitis, pancreatic mass, and lower gastrointestinal bleed. J Clin Gastroenterol 28:364–367
18. Taniguchi T, Seko S, Azuma K, et al. (2001) Autoimmune pancreatitis detected as a mass in the head of the pancreas with contiguous fibrosis around the superior mesenteric artery. Dig Dis Sci 46:187–191
19. Horiuchi A, Kaneko T, Yamamura N, et al. (1996) Autoimmune chronic pancreatitis simulating pancreatic lymphoma. Am J Gastroenterol 91:2607–2609
20. Wakabayashi T, Kawaura Y, Satomura Y, et al. (2003) Clinical and imaging features of autoimmune pancreatitis with focal pancreatic swelling or mass formation: comparison with so-called tumor-forming pancreatitis and pancreatic carcinoma. Am J Gastroenterol 98:2679–2687